DISTRIBUTION OF PERIODIC ORBITS FOR THE CASATI-PROSEN MAP ON RATIONAL LATTICES

NATASCHA NEUMÄRKER, JOHN A. G. ROBERTS, AND FRANCO VIVALDI

Abstract. We study numerically the periodic orbits of the Casati-Prosen map, a two-parameter reversible map of the torus, with zero entropy. For rational parameter values, this map preserves rational lattices, and each lattice decomposes into periodic orbits. We consider the distribution function of the periods over prime lattices, and its dependence on the parameters of the map. Based on extensive numerical evidence, we conjecture that, asymptotically, almost all orbits are symmetric, and that for a set of rational parameters having full density, the distribution function approaches the gamma-distribution $\mathcal{R}(x) = 1 - e^{-x}(1 + x)$. These properties, which have been proved to hold for random reversible maps, were previously thought to require a stronger form of deterministic randomness, such as that displayed by rational automorphisms over finite fields. Furthermore, we show that the gamma-distribution is the limit of a sequence of singular distributions which are observed on certain lines in parameter space. Our experiments reveal that the convergence rate to $\mathcal{R}$ is highly non-uniform in parameter space, being slowest in sharply-defined regions reminiscent of resonant zones in Hamiltonian perturbation theory.

1. Introduction

This paper is concerned with the distributional properties of the periodic orbits of a zero-entropy reversible map —the Casati-Prosen triangle map [3, 8]— and the extent to which such properties are the same as those of random reversible maps. This work is part of ongoing research on reversibility in a discrete setting [16, 17, 12]

A map L is said to be *reversible* if it is the composition of two involutions G and $H = L \circ G$. The involution G conjugates the map to its inverse, namely

$$G \circ L \circ G \;=\; L^{-1} \qquad\qquad G^2 = Id. \tag{1}$$

Any G that satisfies (1) is called a *reversing symmetry* for L. (For background information on reversibility, see [10, 11, 14], and references therein.)

We consider reversible twist maps of the so-called generalised standard form

$$L : x' = x + y', \qquad\qquad y' = y + f(x), \tag{2}$$

We regard L as a map of $\mathbb{R}^2$ or $\mathbb{C}^2$, or indeed of $\mathbb{F}^2$, where $\mathbb{F}$ is any field. If f is periodic, then L commutes with a discrete group of translations, and may be reduced to map of the cylinder or the torus. The map L is reversible for any choice of the function f, since we can write $L = H \circ G$, where

$$G : x' = x, \quad y' = -y - f(x) \qquad\qquad H : x' = x - y, \quad y' = -y. \tag{3}$$

One verifies that G and H are orientation-reversing involutions. The family (2) includes well-known maps such as the Chirikov-Taylor standard map of the cylinder or torus, for which $f(x) = \alpha \sin(x)$, and the area-preserving Hénon map of the plane, corresponding to

$f(x) = x^2 + \alpha$. In this paper we specialize the map L to the Casati-Prosen (C-P) triangle map T of the two-dimensional torus $\mathbb{T}^2$, for which the function f is given by [8]:

$$f(x) = \alpha\,\theta(x) + \beta \qquad\qquad \theta(x) = \begin{cases} 1 & x \in [0, \frac{1}{2}) \\ -1 & x \in [\frac{1}{2}, 1). \end{cases}$$

Both variables x and y are periodic with period 1, and the parameters α, β are real numbers. The C-P map has zero entropy, being piecewise parabolic, and it is conjectured to be uniquely ergodic and mixing for almost all choices of parameters. However, these properties appear to be very difficult to establish rigorously [8]. There is a growing interest in the ergodic-theoretic properties of two-dimensional maps with zero entropy, stimulated by recent developments in the one-dimensional case [1].

In this paper we focus our attention on the rational periodic orbits of the C-P map. This map has no periodic orbits at all if $\beta \notin \mathbb{Z} + \alpha\mathbb{Z}$ [8, lemma 1], and this condition requires that at least one of α, β is irrational. If, on the other hand, both parameters are rational, then all rational points on the torus are periodic. To see this, we consider the orthogonal rational lattice Λ_N on the torus, with N^2 points

$$\Lambda_N \;=\; \left\{ \left(\tfrac{k}{N}, \tfrac{\ell}{N}\right) \,|\, 0 \le k, \ell < N \right\} \qquad N \in \mathbb{N}. \tag{4}$$

Then we let

$$\gamma = \beta + \alpha \qquad\qquad \delta = \beta - \alpha. \tag{5}$$

From an algebraic viewpoint, the parameters γ, δ are more natural than α and β; the latter, however, are more significant dynamically. We will use both, as appropriate.

The map T preserves Λ_N if and only if $(\gamma, \delta) \in \Lambda_N$; if α and β are rational, then, without loss of generality, we may assume that this is the case. All orbits of T over Λ_N are periodic, being the orbits of an invertible map over a finite set. We can therefore consider the distributional properties of their periods, which we characterise by means of the period distribution function

$$\mathcal{D}_N(x) = \frac{\#\{z \in \Lambda_N \,:\, t(z) \leqslant \kappa x\}}{N^2} \tag{6}$$

where $t(z)$ is the minimal period of the point z, and the constant κ is a normalisation parameter to be determined below. The function $\mathcal{D}_N$, which depends of α and β, is a step function, with the number of steps being equal to the number of distinct periods of T over Λ_N at the chosen parameter values.

Given that every invertible map of a finite space is reversible, albeit in a trivial sense [16], developing a meaningful characterisation of reversibility for discrete systems requires the study of asymptotic phenomena. In a series of papers [15, 16, 17, 12], we have investigated the limiting (large N) properties of period distribution functions for various algebraic maps of finite phase spaces, including the area-preserving Hénon map. If these maps have a single family of reversing symmetries[1], and act on the space $\Lambda_p = \mathbb{F}_p^2$, where $\mathbb{F}_p$ is the finite field with p elements (p a prime), then we conjectured that

$$\lim_{p\to\infty} \mathcal{D}_p(x) = \mathcal{R}(x) = 1 - e^{-x}(1 + x) \qquad x \geqslant 0 \tag{7}$$

where the normalisation constant κ is the mean period $\bar{t}$ of the orbits, that is,

$$\kappa = \bar{t} = \frac{N^2}{\#\text{cycles}}. \tag{8}$$

[1]This means that there exists G satisfing equation (1), and that L commutes only with its own iterates.

(In this paper, the terms 'cycle' and 'periodic orbit' are used interchangeably.) The function $\mathcal{R}$ is the distribution function of the gamma-density with shape and scaling parameters equal to 2 and to 1, respectively [9]. This distribution was shown to be the limiting period distribution of the composition of two random involutions, with some (mild) conditions on the cardinalities of the respective fixed sets [17, theorem A]. The normalisation (8) appears naturally in this context, because the number of cycles is closely connected to the cardinality of the fixed sets of the involutions. Indeed, in the typical case in which both fixed sets have N points, there are exactly N symmetric cycles, and $\sim N$ cycles.

The above findings suggest that convergence to the gamma-distribution (7) provides a meaningful characterisation of reversibility over a finite space. We note, however, that the limit (7) has not been established rigorously for any deterministic map. (Note that in the absence of reversibility, the period distribution differs drastically. Upon scaling by $\kappa = N^2$, the function $\mathcal{D}_N$ for a random invertible map converges to the identity function on the unit interval.)

In the case of the family (2), a natural question is to identify minimal requirements on f which suffice to observe the asymptotics (7). We have noted that, over a finite field, the choice $f(x) = x^2+c$ (the Hénon map) is believed to give the gamma-distribution. By contrast, we will show below —see section 3— that the function $f(x) = \beta$ generates a step-like distribution, meaning that, asymptotically, the (normalised) periods of the orbits assume a discrete set of values. Singular distributions appear also for linear functions $f(x) = cx$, $c \in \mathbb{N}$, which correspond to hyperbolic toral automorphisms [13]. In this case the lattice dynamics is given by the action of finite abelian groups, which accounts for the quantisation of periods. The C-P map, for which f is piecewise constant, may be considered as a minimal departure from the cases mentioned above, and this justifies our interest in this model. A study of a special case of the C-P map over rational lattices Λ_N was carried out in [18]. At the chosen parameter values ($\beta = 0$, $\alpha = 1/N$), this map is a discrete version of a near-integrable twist map; it has a very rich dynamics, and its period distributions are quite different from (7). Thus, even within the context of rational parameters, we have to exclude 'exceptional' parameter values. This is one of the themes of this work.

Our main concern is the convergence properties of the distributions $\mathcal{D}_N$ for the C-P map in the case in which $N = p$ is a prime number. The prime lattices Λ_p have no non-trivial invariant sub-lattices, which avoids the appearance of spurious symmetries, and improves convergence. Furthermore, in the presence of singular distributions, the restriction to prime lattices invariably leads to neater results, because the location of the singularities of these distributions appears to depend on the proper divisors of the denominator.

A considerable amount of information is gathered by examining the norm of the difference $\mathcal{D}_p - \mathcal{R}$, as a function of the parameters of the map, for a large prime p (figure 1).

Our findings are summarised informally as follows.

As $p \to \infty$, we observe the following:

1. *For almost all parameters values, the norm of the difference $\mathcal{D}_p - \mathcal{R}$ converges to zero.*
2. *For $k = 1, 2, \ldots$, if $\beta = k\alpha$, then the period distribution converges to a singular distribution $\mathcal{R}^{(k)}$ (see below), with the property that $\lim_{k\to\infty} \mathcal{R}^{(k)} = \mathcal{R}$.*
3. *Almost all rational periodic points are symmetric (i.e., G-invariant).*

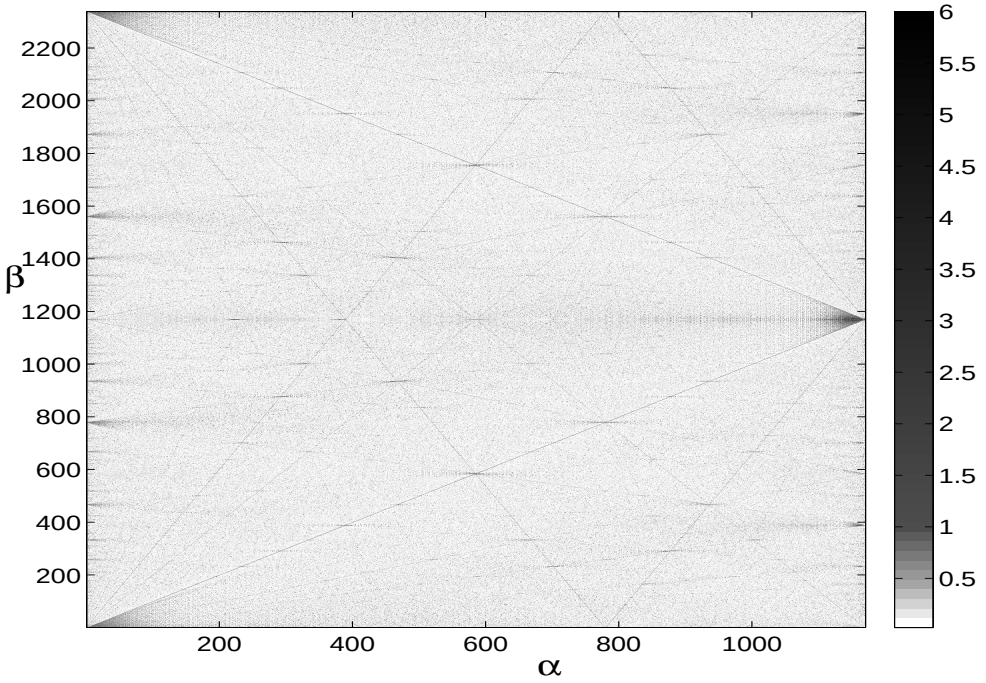

Figure 1: Parameter space of the C-P map for $N = p = 2339$, a prime number, each pixel representing a parameter pair (α, β). The value of the norm of the difference $\mathcal{D}_p(\alpha, \beta) - \mathcal{R}$ (equation (15)) is coded on a grey scale, the darker a pixel, the larger the deviation from the gamma-distribution (7). Two blow-ups of this image are shown in figure 4; for parameters (α, β) near $(0, 0)$ (left frame, for the larger prime $p = 9011$), and near $(1/4, 1/4)$ (right frame, for the prime $p = 11433$).

For even k, the distribution $\mathcal{R}^{(k)}$ is given explicitly as

$$\mathcal{R}^{(k)}(x) = \sum_{j=1}^{n(x)} \frac{j(k-1)^{j-1}}{k^{j+1}} \qquad n(x) = \lceil kx \rceil - 1, \qquad k = 2, 4, 6, \ldots .$$

We have only incomplete knowledge of $\mathcal{R}^{(k)}$ for odd k —see section 3.2.

These statements will be formulated precisely in section 3 as conjectures 1–3, and our goal is to provide supporting evidence. While gathering evidence, we shall discover that the rate of convergence of averages is highly non-uniform in parameter space. The regions with the slowest convergence have a remarkable structure, reminiscent of resonant zones in Hamiltonian perturbation theory. This phenomenon is visible in figure 1.

The computations described in this paper are substantial. They involve the numerical exploration of the asymptotic (large p) properties of a family of maps over a two-dimensional lattice with p^2 points. In addition, there are p^2 possible choices of parameter pairs, and therefore the computational time grows proportionally to p^4. The slow convergence of averages complicates matters further. Essential savings in storage were achieved by exploiting the

dominance of symmetric orbits mentioned above, while computational time was cut by a half by using an additional symmetry in parameter space (see figure 1 and section 2).

The plan of the paper is as follows. In section 2 we establish the reversibility properties of the C-P map, together with the symmetry in parameter space mentioned above (lemma 1). In section 3 we formulate our conjectures precisely, and prepare the analytical set-up necessary for the experiments. In particular, we establish the presence of singular distribution on some rational lines (proposition 2). In section 4 we describe our numerical experiments, centred on the analysis of the norm of the differences $\mathcal{D}_p - \mathcal{R}$ and $\mathcal{R}_p^{(k)} - \mathcal{R}^{(k)}$ between empirical (subscript p) and conjectured distribution functions. We also keep track of the fraction of the space occupied by symmetric orbits. Finally, in section 5 we offer concluding remarks.

2. Reversibility and symmetry of the Casati-Prosen map

The family of maps (2) can be written as the composition of two shears, one in y followed by one in x, that is, $L = S_x \circ S_y$, where

$$\begin{aligned} S_y &: x' = x, \quad y' = y + f(x) \\ S_x &: x' = x + y, \quad y' = y. \end{aligned}$$

We have pointed out that these maps are reversible for any choice of f, with the involutions G and H given by (3). Because these involutions are orientation-reversing (their Jacobian determinant is equal to -1), their fixed sets $Fix(G)$ and $Fix(H)$ —the so-called *symmetry lines*— are one-dimensional [5]. The symmetry lines of the involutions (3) are given by

$$Fix(G) = \{(x, y) : 2y = -f(x)\} \qquad Fix(H) = \{(x, 0)\}, \tag{9}$$

where f is arbitrary.

Consider now the *symmetric* periodic orbits, namely those orbits of L invariant under G (and hence also invariant under $H = L \circ G$). These orbits are determined uniquely by their intersections with the symmetry lines [4]. More precisely, a symmetric periodic orbit with odd period $2k-1$ has one point (x, y) on the symmetry line $Fix(G)$ and one point $L^k(x, y)$ on $Fix(H)$. One of even period $2k$ has two points (x, y) and $L^k(x, y)$ both on $Fix(G)$ or both on $Fix(H)$. The ability to find symmetric periodic orbits by searching along the one-dimensional symmetry lines gives a considerable advantage compared to finding asymmetric periodic orbits, which requires a two-dimensional search.

Specialising equations (2) and (9) to the C-P map T (4), we have:

$$\begin{array}{ll} G : x' = x, \quad y' = -y - \alpha\,\theta(x) - \beta & Fix(G) : \{(x, y) : 2y = -\alpha\,\theta(x) - \beta\} \\ H : x' = x - y, \quad y' = -y & Fix(H) : \{(x, 0)\}. \end{array} \tag{10}$$

For rational parameters α and β, we consider the action of T over the lattice Λ_N, given in (4), where N is the least common denominator of α and β. Clearing denominators in (4), we obtain the integer lattice of the numerators, which we still denote by Λ_N. The action of $T \pmod 1$ on this invariant integer lattice can now be described by the permutation T_N, given by

$$T_N : x' \equiv x + y' \pmod N \qquad y' \equiv y + \alpha\,\theta_N(x) + \beta \pmod N \tag{11}$$

where we now abuse notation by identifying x, y, α and β with their respective numerators over the common denominator N, so in (11)

$$x, y, \alpha, \beta \in \{0, 1, 2, \ldots N-1\},$$

and

$$\theta_N(x) = \begin{cases} 1 & x \in \{0, 1, \ldots, \lceil N/2 \rceil - 1\} \\ -1 & x \in \{\lceil N/2 \rceil, \ldots, N-1\}. \end{cases}$$

The permutation T_N inherits the corresponding reversibility (10) with now:

$$\begin{array}{rcl} Fix(H) & = & \{(x,0) \,:\, x = 0, \ldots, N-1\} \\ Fix(G) & = & \{(x,y) \,:\, 2y \equiv -\alpha\,\theta_N(x) - \beta \,(\mathrm{mod}\ N)\} \end{array} \tag{12}$$

Now $Fix(H)$ and $Fix(G)$ are finite sets, with $Fix(H)$ being a line with N lattice points. When N is odd, the integer 2 has a modular inverse, and $Fix(G)$ is the union of two 'half-lines' on the lattice, the $\lceil N/2 \rceil$ lattice points with height $y \equiv -(\alpha+\beta)/2 \,(\mathrm{mod}\ N)$ on the left, and the $\lfloor N/2 \rfloor$ lattice points with height $y \equiv (\alpha-\beta)/2 \,(\mathrm{mod}\ N)$ on the right. In this case,

$$(\#Fix\,G + \#Fix\,H)/2 = N$$

and by [16, Lemma 1], there are precisely N symmetric cycles. When N is even, $Fix(G)$ is empty if $\alpha + \beta \,(\mathrm{mod}\ N)$ is odd, and there are exactly $N/2$ symmetric cycles. When N and $\alpha + \beta \,(\mathrm{mod}\ N)$ are both even, then

$$Fix(G) = \{(x, -(\alpha\,\theta_N(x) + \beta)/2 \,(\mathrm{mod}\ N/2))\} \cup \{(x, -(\alpha\,\theta_N(x) + \beta)/2 \,(\mathrm{mod}\ N/2) + N/2)\},$$

that is, four 'half-lines' on the lattice, so again there are N symmetric cycles.

In the next section, we study the dynamics of T_N over the entire parameter space $\{(\alpha, \beta) : \alpha, \beta \in \{0, 1, 2, \ldots N-1\}\}$. Using $T_N^{\alpha,\beta}$ to highlight the explicit dependence of T_N on its parameters, we have

Lemma 1. *For odd N, the maps $T_N^{\alpha,\beta}$ and $T_N^{-\alpha,-\beta}$ are conjugate permutations of the N^2 points of Λ_N, hence have the same cycle structure. For even N, the same is true for $T_N^{\alpha,\beta}$, $T_N^{-\alpha,-\beta}$ and $T_N^{-\alpha,\beta}$ —they are all conjugate on Λ_N— and $T_N^{\alpha,\beta} = T_N^{\alpha+N/2,\beta+N/2}$.*

Proof. Consider the invertible change of coordinates $\Phi : x = aX + b$, $y = aY$. With $a = \pm 1$, Φ also defines an invertible map of the torus. The transformed version of T is then:

$$\Phi^{-1} \circ T \circ \Phi : X' = X + Y', \qquad Y' = Y + \frac{1}{a}[\alpha\,\theta(aX + b) + \beta]. \tag{13}$$

For the choice $a = -1$, $b = \lfloor N/2 \rfloor$, we have

$$\Theta(X) := \frac{1}{a}[\theta(aX + b)] = -\theta(X) \tag{14}$$

because of the invariance $\theta(x) \equiv \theta(-x + \lfloor N/2 \rfloor) \,(\mathrm{mod}\ N)$ for odd or even N. Consequently, with these choices of a and b,

$$\Phi^{-1} \circ T_N^{\alpha,\beta} \circ \Phi = T_N^{-\alpha,-\beta},$$

showing that a change of sign in parameters makes $T_N^{\alpha,\beta}$ and $T_N^{-\alpha,-\beta}$ conjugate permutations for any N. For N even, additionally one has $\theta(x) \equiv -\theta(x + N/2) \,(\mathrm{mod}\ N)$, corresponding to taking the choice $a = 1$, $b = N/2$ in (14), so $T_N^{\alpha,\beta}$ and $T_N^{-\alpha,\beta}$ are also conjugate permutations. The last statement of the lemma for N even is obvious. □

From this lemma it follows that, for N even, one need only consider parameters lying in the triangle with vertices $(0,0)$, $(N/2, 0)$, and $(N/2, N/2)$. If N is odd, then $\theta(x)$ and $-\theta(x + \lceil N/2 \rceil) \,(\mathrm{mod}\ N)$ agree on all sites except $x = \lceil N/2 \rceil - 1$ when the former gives $+1$

and the latter gives -1. Thus for large odd N, there is an approximate symmetry between the maps $T_N^{-\alpha,\beta}$ and $T_N^{\alpha,\beta}$ —see figure 1.

3. Characterising convergence

In this section we formulate precisely the conjectures mentioned in the introduction, and develop the analysis that will support the computations described in the next section.

3.1. **Convergence to the gamma-distribution.** We consider the convergence properties of the empirical distributions $\mathcal{D}_p$ given in (6), for the C-P map on the prime lattice Λ_p (see equation (4)). The parameters have the same prime denominator, $(\alpha,\beta) \in \Lambda_p$, and to make the parameter dependence explicit, we use the notation $\mathcal{D}_{p,\alpha,\beta}$. We want to determine whether or not convergence of $\mathcal{D}_p$ to the gamma-distribution (7) will occur for a typical choice of parameters.

To make this idea precise, we first introduce the quantity

$$\mathcal{E}_p(\alpha,\beta) = \int_0^\infty |\mathcal{D}_{p,\alpha,\beta}(x) - \mathcal{R}(x)|\, dx \tag{15}$$

which measures the distance of the distribution $\mathcal{D}_{p,\alpha,\beta}$ (with scaling constant (8)) from $\mathcal{R}$ in the L^1-norm.

Now fix a real constant $c > 0$, and consider the function

$$E_p(c) = \frac{\#\{(\alpha,\beta) \in \Lambda_p \,:\, \mathcal{E}_p(\alpha,\beta) < c\}}{p^2}. \tag{16}$$

This is the proportion of rational parameter pairs with common denominator p, for which the period distribution function lies at distance smaller than c from $\mathcal{R}$. For fixed p, the function $E_p(c)$ is a distribution function: it is non-decreasing, and it is equal to 1 for all sufficiently large c. Then we define

$$E(c) = \liminf_{p\to\infty} E_p(c) \qquad c > 0. \tag{17}$$

The function E is non-decreasing. Numerical evidence suggests that E has a much stronger property:

Conjecture 1. *The function E is identically equal to 1.*

This conjecture states that the period distribution of the rational cycles of the C-P map, is, for almost all rational parameters with prime denominator, the same as that of a random reversible map [17]. The convergence of E_p to 1 is necessarily non-uniform, because for any finite p, the value of $E_p(c)$ must be zero in a small neighbourhood of the origin. We shall see that, in addition, the convergence is very slow.

By construction, the function E is not affected by contributions from possible 'anomalous' distributions, which may appear for sets of parameters of size $o(p^2)$. A class of anomalous distribution is found over lines in parameter space with (low-order) rational slope; we deal with them in the next section. A second class of anomalous distributions appears in certain two-dimensional regions in parameter space, located in the vicinity of low-order rationals.

3.2. **Singular distributions on rational lines.** An infinite sequence of anomalous distributions originates from parameters of the form $\beta = k\alpha$, for $k = 1, 2, \ldots$. These are singular distributions, whose asymptotic properties appear to depend only on k. Moreover, it turns out that, in the limit of large k, these distributions converge to the gamma-distribution (see below). Thus, within a single family of maps, one can observe the transition from a singular orbit statistics to the smooth orbit statistics of random reversible maps.

We begin with a simple case, which can be treated exactly. We define the step-functions

$$\mathcal{D}_1(x) = \begin{cases} 0 & \text{if } x < 1 \\ 1 & \text{if } x \geqslant 1 \end{cases} \tag{18}$$

$$\mathcal{D}_p^{(m)}(x) = \begin{cases} 0 & \text{if } 0 \leqslant x < \frac{1}{p^m} \\ \frac{1}{p^i} & \text{if } \frac{1}{p^i} \leqslant x < \frac{1}{p^{i-1}}, \quad i = 1, 2, \ldots, m \\ 1 & \text{if } x \geqslant 1. \end{cases} \tag{19}$$

The following results establishes the limiting behaviour of the empirical distribution function $\mathcal{D}_{N,\alpha,\beta}$ for some special choice of parameters. In order to achieve simple limiting distributions, we shall adopt a normalisation distinct from (8).

Proposition 2. *Let $N = p^n$ be a prime power, let $(\alpha, \beta) \in \Lambda_{p^n}$, with $\alpha = 0$, and let $x \geqslant 0$. Build the distribution* (6) *with $\kappa = N = p^n$.*

For $\beta = 0$ the following holds:

$$\lim_{p\to\infty} \mathcal{D}_{p^n,0,0}(x) = \mathcal{D}_1(x) \tag{20}$$

$$\lim_{n\to\infty} \mathcal{D}_{p^n,0,0}(x) = \mathcal{D}_p^{(\infty)}(x). \tag{21}$$

For $\beta > 0$, and p odd, we have

$$\begin{aligned} \lim_{p^n\to\infty} \mathcal{D}_{p^n,0,\beta}(x) &= \mathcal{D}_1(x) \qquad \gcd(\beta, p) = 1 \\ \lim_{p\to\infty} \mathcal{D}_{p^n,0,\beta}(x) &= \mathcal{D}_1(x) \qquad \gcd(\beta, p) \neq 1 \\ \lim_{n\to\infty} \mathcal{D}_{p^n,0,\beta}(x) &= \mathcal{D}_p^{(m)}(x) \qquad \beta = p^m \qquad m = 1, \ldots, n-1. \end{aligned} \tag{22}$$

(The case $p = 2$ is omitted for the sake of brevity.)

Proof. When $\alpha = 0$, the C-P map is

$$x' \equiv x + y' \pmod N \qquad y' \equiv y + \beta \pmod N. \tag{23}$$

and the t-th iterate of an initial point (x_0, y_0) is given by

$$x_t \equiv x_0 + y_0 t + \frac{\beta}{2} t(t+1) \pmod N \qquad y_t \equiv y_0 + \beta t \pmod N. \tag{24}$$

Consider firstly $\beta = 0$. Then the map (23) is an integrable twist map modulo N. Indeed every line $y = y_0$ is invariant, and on each line the x-dynamics is a translation, namely the y_0-fold composition of the generating translation $x' = x + 1$. These translations represent the full ensemble of N possible translations modulo N.

From equation (23), the period of the point (x_0, y_0) is given by the smallest positive solution t to the congruence $y_0\, t \equiv 0 \,(\mathrm{mod}\ N)$. Simplification yields

$$t\frac{y_0}{d} \equiv 0 \,(\mathrm{mod}\ \frac{N}{d}) \qquad d = \gcd(y_0, N), \tag{25}$$

giving the period $t = N/d$, independent of x_0, and there are d orbits with that period.

For every divisor d of N, the number of lines $y = y_0$ such that $\gcd(y_0, N) = d$ is equal to $\phi(N/d)$ where ϕ is Euler's totient function. In particular, the choice $d = N$ ($y_0 = 0$) gives a single line with N fixed points for the map. If $N = p$ is prime, the only other possibility is $d = 1$, corresponding to $p - 1$ lines each containing one orbit of maximal period $t = N$. For general N, the N^2 points of Λ_N are accounted for courtesy of the divisor sum [7, Theorem 63]

$$\sum_{d|N} d\frac{N}{d}\phi\left(\frac{N}{d}\right) = N\sum_{d|N}\phi\left(\frac{N}{d}\right) = N\sum_{d|N}\phi(d) = N^2.$$

For every divisor t of N, the number of points of period t is $N\phi(t)$, and hence the fraction $\mu(t)$ of phase space occupied by points of period at most t is equal to

$$\mu(t) = \frac{1}{N}\sum_{\substack{t'|N\\ t'\le t}}\phi(t'). \tag{26}$$

Specializing to $N = p^n$, we have the periods $t_i = p^i$ ($i = 0, \dots, n$), and the sum (26) becomes

$$\mu(p^i) = \frac{1}{p^n}\sum_{j=0}^{i}\phi(p^j) = p^{i-n}.$$

We consider the limit of large N with n fixed and $p \to \infty$. The natural period normalization is N, consistent with the map (23) with $\beta = 0$ being an ensemble of N translations. Taking $\kappa = N$ gives the distribution (20).

Next we take p fixed and $n \to \infty$. Normalizing periods by N, the proportion of phase space consumed in cycles with normalized period less than or equal to p^i/p^n is p^i/p^n for $i = 0, 1, \dots, n$, leading to (21).

Consider now the case of (23) when $\beta > 0$. From the second equation in (24), a necessary condition for an orbit to be periodic is $\beta t \equiv 0 \,(\mathrm{mod}\ N)$, independent of y_0. By analogy with equation (25) above, we find that the smallest positive solution is $t = \tau = N/r$ where $r = \gcd(\beta, N)$. From (24), we obtain the time-τ map

$$x_\tau \equiv x_0 + y_0\tau + \frac{\beta}{2}\tau(\tau+1) \pmod N \qquad y_\tau \equiv y_0 \pmod N. \tag{27}$$

The y-component is constant, while the x-component is a translation by U, where

$$U = U(y_0) \equiv y_0\tau + \frac{\beta}{2}\tau(\tau+1) \,(\mathrm{mod}\ N).$$

It follows that all orbits of (24) have period equal to a multiple of τ, the multiple being the additive order of U modulo N, which is N/s where $s = s(y_0) = \gcd(U, N)$. We see that when $\beta > 0$, the N horizontal lines are partitioned into r invariant sets, each consisting of τ lines, for a total of τN points. These points are consumed in s cycles of period $\tau N/s$.

Several cases arise:

(i) If β is coprime to N and N is odd, then $r = 1$, $\tau = N$ and $U \equiv 0 \,(\mathrm{mod}\ N)$, independent of x_0 and y_0. The x_τ-translation is the identity, $s = N$, and the C-P map (23) has N orbits of period N.

(ii) If β is coprime to N and N is even, then $r = 1$, $\tau = N$ and $U \equiv \beta N/2 \,(\mathrm{mod}\, N)$, independent of x_0 and y_0. We have $s = N/2$, and the C-P map has $N/2$ orbits of period $2N$.
(iii) If $\gcd(\beta, N) = r > 1$ and $\tau = N/r$ is odd, then $U \equiv y_0\tau \,(\mathrm{mod}\, N)$. Then $s = \gcd(y_0\tau, r\tau) = \tau \gcd(y_0, r)$, contributing a period $N/\gcd(y_0, r) = \tau r/\gcd(y_0, r)$ for the C-P map.
(iv) If $\gcd(\beta, N) = r > 1$ and $\tau = N/r$ is even, then $U \equiv y_0\tau + \beta\tau/2 \,(\mathrm{mod}\, N)$. Then $s = \gcd(y_0\tau + \beta\tau/2, r\tau) = (\tau/2)\, \gcd(2y_0 + \beta, 2r)$, contributing a period $2N/\gcd(2y_0 + \beta, 2r) = 2\tau r/\gcd(2y_0 + \beta, 2r)$ for the C-P map.

We specialize to $N = p^n$ with p odd. If β and N are coprime (that is, $\beta \neq p^m$, $m = 1, \ldots, n-1$), then case (i) above applies, yielding the distribution $\mathcal{D}_1(x)$ in the limit $N \to \infty$ with p fixed or n fixed. Otherwise, if $\beta = p^m$, then case (iii) applies with $r = \beta$. Normalizing periods by N, the allowable normalised periods take the form $1/\gcd(y_0, p^m) = p^{-l}$, $l = 0, \ldots, m$, consuming proportions of phase space equal to $p^{-m}\phi(p^m/\gcd(y_0, p^m)) = (1 - p^{-1})p^{-l}$, for $l < m$, and to p^{-m} for $l = m$. This reverts to the problem considered above, and the corresponding distribution functions in the remaining two limits in (22). □

Remark 1. The above proposition raises the question as to the choice of an appropriate normalisation parameter for the distribution function (6). In the case of the gamma-distribution (7), one verifies that the expectation value $\langle x \rangle$ of the normalised period with respect to the associated gamma-density xe^{-x} is equal to 1. This implies that the expected period $\langle t \rangle$ is equal to the mean period $\bar{t}$ given in (8).

This is no longer the case for the singular distributions of proposition 2, as we now show. When $\alpha = \beta = 0$, the number of periodic orbits of minimal period t (or *t-cycles*) of the C-P map over Λ_N is equal to

$$\#t\text{-cycles} = \frac{N}{t}\phi(t) = \begin{cases} N & \text{if } t = 1 \\ N \prod_{p|t} \left(1 - p^{-1}\right) & \text{if } t > 1 \end{cases} \tag{28}$$

where the product is taken over all prime divisors p of t. Hence the mean cycle length $\bar{t}$, given in equation (8), is

$$\bar{t} = \frac{N^2}{\#\text{cycles}} = \frac{N}{1 + \sum_{\substack{t|N \\ t>1}} \prod_{p|t} \left(1 - p^{-1}\right)}. \tag{29}$$

As noted above, the number of points of period t over Λ_N is equal to $N\phi(t)$ if t divides N, and zero otherwise. It follows that the expectation value $\langle t \rangle$ for the period, with respect to the uniform measure on Λ_N, is given by

$$\langle t \rangle = \sum_{t|N} t\, \frac{\phi(t)}{N}. \tag{30}$$

Specialising the above quantities to the parameters $N = p^n$, we find

$$\begin{aligned} \bar{t} &= \frac{p^n}{1 + \sum_{j=1}^{n} (1 - p^{-1})} = \frac{p^{n+1}}{p(n+1) - n} \\ \langle t \rangle &= \sum_{i=0}^{n} p^i \frac{\phi(p^i)}{p^n} = \frac{1}{p^n} + \frac{p-1}{p^{n+1}} \sum_{i=1}^{n} p^{2i} = \frac{1}{p^n} + \frac{1}{p^{n-1}} \frac{p^{2n} - 1}{p + 1}. \end{aligned}$$

In the limit of large N with n fixed and $p \to \infty$, we have

$$\bar{t} \sim \frac{N}{n+1} \qquad \langle t \rangle \sim N.$$

In this case the scaling parameter $\kappa = N = \langle t \rangle$ gives the simple limiting distribution $\mathcal{D}_1$, whereas the choice $\kappa = \bar{t}$ would lead to a shifted singularity.

If instead we take p fixed and $n \to \infty$, we find

$$\bar{t} \sim \frac{N}{\log_p(N)} \frac{p}{p-1} \qquad \langle t \rangle \sim N \frac{p}{p+1}.$$

Here the presence of the logarithmic term in $\bar{t}$ would shift the singularities of $\mathcal{D}_p^{(m)}$ to infinity.

Remark 2. When $\alpha = 0$ in the C-P map, many additional reversing symmetries are present because the C-P map has many non-trivial commuting maps. When $\alpha = \beta = 0$, the x translation on any line, $x' = x + y_0$, commutes with any other translation on that line and has the involution $x' = -x$ as a reversing symmetry. Consequently, the C-P map on Λ_N with $\alpha = \beta = 0$ commutes with any map $S_u : x' \equiv x + u(y) \,(\mathrm{mod}\ N),\ y' \equiv y \,(\mathrm{mod}\ N)$, where u is any integer-valued function, and has the reversing symmetry $R : x' \equiv -x \,(\mathrm{mod}\ N),\ y' \equiv y \,(\mathrm{mod}\ N)$. The latter is a different reversing symmetry to G of (10). Taken together, commuting maps and reversing symmetries for a given map form a group, the so-called *reversing symmetry group* [2]. For instance, the composition of two reversing symmetries commutes with the map, so we see that $R \circ G : x' = -x, y' = -y$ also commutes with C-P with $\alpha = \beta = 0$. When $\alpha = 0$ but $\beta \neq 0$, the proof above shows that the τ-th iterate of the C-P map again reduces to x-translations on each horizontal line, and then inherits the aforementioned commuting maps and reversing symmetries (in this case, we say that the C-P map has (reversing) τ-symmetries [2]). The appearance of the gamma-distribution (7) has been confined to maps that have no nontrivial commuting maps (other than their powers) and a single generating reversing symmetry.

Remark 3. The case $\alpha = \beta = 0$ of the C-P map is equivalent to the action of the *parabolic* integer matrix $\left(\begin{smallmatrix} 1 & 1 \\ 0 & 1 \end{smallmatrix}\right)$ on Λ_N. The action of *hyperbolic* integer matrices on Λ_N, and their related singular period distributions, is a well-studied topic [13].

We return to the C-P map for general α, β. To deal with anomalous distributions on lines, we consider the following sequence of functions

$$\mathcal{R}^{(k)}(x) = \sum_{j=1}^{n(x)} \frac{j(k-1)^{j-1}}{k^{j+1}} \qquad n(x) = \lceil kx \rceil - 1, \qquad k = 2, 4, 6, \ldots. \tag{31}$$

For $x \leqslant 1/k$ the sum is empty, and $\mathcal{R}^{(k)}$ is defined to be zero. These are step-functions, with steps at the integer multiples of k^{-1}. The index k is restricted to even values because for odd k these functions are not relevant to the periodic orbits of the C-P map. The functional form of these singular distributions was determined by trial and error, by matching the result of accurate numerical experiments (see section 4). At the end of this section, we offer a heuristic argument to justify the location of the singularities of these distributions.

Next we show that the functions $\mathcal{R}^{(k)}$ are distribution functions that converge to the gamma-distribution as $k \to \infty$. For each k, the function $\mathcal{R}^{(k)}$ is non-negative and non-decreasing; to show that $\mathcal{R}^{(k)}$ is a distribution function we must verify that $\lim_{x\to\infty} \mathcal{R}^{(k)}(x) = 1$.

Lemma 3. *The following holds*

$$\lim_{x\to\infty} \mathcal{R}^{(k)}(x) = 1 \qquad \lim_{k\to\infty} \mathcal{R}^{(k)}(x) = \mathcal{R}(x), \quad x \geqslant 0.$$

PROOF. Using the derivative of the geometric series to evaluate the sum, one obtains

$$\begin{aligned}\sum_{j=1}^{n} \frac{j(k-1)^{j-1}}{k^{j+1}} &= \frac{1}{k^2} \cdot \frac{n\left(\frac{k-1}{k}\right)^{n+1} - (n+1)\left(\frac{k-1}{k}\right)^{n} + 1}{(\frac{k-1}{k} - 1)^2} \\ &= 1 - \left(1 - \frac{1}{k}\right)^{n+1} \left(\frac{k}{k-1} + \frac{n}{k-1}\right).\end{aligned}$$

Using (31), and noting that $n(x) = kx + O(1)$, we obtain

$$\lim_{x\to\infty} \mathcal{R}^{(k)}(x) = 1 - \lim_{n\to\infty} \left(1 - \frac{1}{k}\right)^{n+1} \left(\frac{k}{k-1} + \frac{n}{k-1}\right) = 1$$

as desired. Likewise, we find

$$\begin{aligned}\lim_{k\to\infty} \mathcal{R}^{(k)}(x) &= 1 - \lim_{k\to\infty} \left(1 - \frac{1}{k}\right)^{kx} \left(1 - \frac{1}{k}\right)^{O(1)} \left(\frac{k}{k-1} + \frac{k}{k-1}x + \frac{O(1)}{k-1}\right) \\ &= 1 - e^{-x}(1+x) = \mathcal{R}(x).\end{aligned}$$

□

Let us now return to the C-P map. We construct a sequence of lines in parameter space, with integer slope, again limiting ourselves to rational numbers with prime denominator $N = p$.

$$\Lambda_p^{(k)} = \{(\alpha, \beta) \in \Lambda_p \setminus \{(0,0)\} \,:\, \beta = k\alpha\} \qquad p \text{ prime}, \quad k = 1, \ldots, p-1.$$

The discrete lines $\Lambda^{(k)}$ are disjoint, and their union is the whole of Λ_p, apart from the set $\alpha\beta = 0$ (the union of two lines). For fixed k, we examine the period distributions for parameter pairs restricted to $\Lambda_p^{(k)}$, and then we let p go to infinity. We shall repeat the procedure used for unconstrained parameter pairs, with the obvious modifications.

We fix a positive real constant c, and consider the quantity

$$E_p^{(k)}(c) = \frac{\#\{(\alpha, \beta) \in \Lambda_p^{(k)} \,:\, \mathcal{E}_p^{(k)}(\alpha) < c\}}{p-1}$$

where the L^1-norm

$$\mathcal{E}_p^{(k)}(\alpha) = \int_0^\infty |\mathcal{D}_{p,\alpha,k\alpha}(x) - \mathcal{R}^{(k)}(x)|\, dx \tag{32}$$

measures the distance between the empirical and the theoretical values.

Finally, we define

$$E^{(k)}(c) = \liminf_{p\to\infty} E_p^{(k)}(c) \qquad c > 0.$$

Numerical evidence suggests the following

Conjecture 2. *For every even integer k, the function $E^{(k)}$ is identically equal to 1.*

Thus letting p and k go to infinity (in that order) we recover the gamma-distribution.

There is a sequence of distributions analogous to (31) for odd k. However, we have been able to identify precisely only the first few terms of this sequence. A restricted version of conjecture 2 for odd k will be given in section 4.

The appearance of singular distributions along the lines $\beta = k\alpha$ can be justified heuristically, assuming ergodicity. From [8, equation (3)], we find, for the t-th iterate of the initial point (x_0, y_0)

$$y_t(x_0, y_0) = y_0 + \beta t + \alpha S_t \qquad\qquad S_t = \sum_{k=0}^{t-1} \theta(x_k).$$

Let $\beta = k\alpha$, for some $k = 1, \ldots, p-1$, and assume that both numerator and denominator of β are co-prime to p. The above equation becomes a congruence modulo p, and for periodicity $(y_t = y_0)$, we require

$$tk + S_t = tk\left(1 + \frac{S_t}{tk}\right) \equiv 0 \,(\mathrm{mod}\ p)$$

to be solved for the smallest $t > 0$. Suppose now that the sequence (x_k) is uniformly distributed in the unit interval. This implies that, as $t \to \infty$, we have $S_t = o(t)$, and hence, asymptotically, kt is an integer multiple of p. After scaling the periods by p, the distribution function approaches a step function, with steps at (some) integer multiples of k^{-1}.

3.3. **Asymmetric orbits.** The C-P map shares another property of random reversible maps, namely the fact that almost all cycles are symmetric. Thus, for rational α and β with common prime denominator p, we consider the proportion $\mathcal{A}_p(\alpha, \beta)$ of points z on the prime lattice Λ_p which belong to asymmetric periodic orbits (this means that $G(z)$ is not in the orbit of z)

$$\mathcal{A}_p(\alpha, \beta) = \frac{\#\{z \in \Lambda_p \,:\, z \text{ belongs to an asymmetric cycle}\}}{p^2}. \tag{33}$$

As done above, we fix a real constant $c \geqslant 0$ and define

$$A_p(c) = \frac{\#\{(\alpha, \beta) \in \Lambda_p \,:\, \mathcal{A}_p(\alpha, \beta) \leqslant c\}}{p^2} \tag{34}$$

which is the fraction of parameter pairs for which the proportion of asymmetric orbits does not exceed c. The function $\mathcal{A}_p$ is non-decreasing, and it is equal to 1 for $c \geqslant 1$. After defining

$$A(c) = \liminf_{p \to \infty} A_p(c) \qquad c \geqslant 0$$

we can formulate our third conjecture.

Conjecture 3. *The function A is identically equal to 1.*

In the rest of the paper, we provide evidence in support of the conjectures stated in this section.

4. Supporting evidence

A typical computation consists of determining the period of all symmetric periodic orbits of the map T on a prime lattice Λ_p, for some large prime number p, and rational parameter pair $(\alpha, \beta) \in \Lambda_p$. This process involves a one-dimensional search along the symmetry lines $Fix(G)$ and $Fix(H)$, given by equation (12). All computations entail integer arithmetic modulo p, as described in section 2.

It turns out that the symmetric orbits occupy nearly all phase space (conjecture 3), and so the total number of iterations of the map is typically very close to p^2. The required storage is only $2p$ —the combined size of the symmetry lines— since there is no need to record the points in the orbits which lie outside the symmetry lines.

From the period data we compute the distribution function $\mathcal{D}_p$, and its distance $\mathcal{E}_p(\alpha,\beta)$ from the gamma-distribution $\mathcal{R}$, or the distance $\mathcal{E}_p^{(k)}(\alpha)$ from the singular distribution $\mathcal{R}^{(k)}$, as appropriate —see equations (15) and (32). In addition, we compute the fraction $\mathcal{A}_p$ of the space occupied by asymmetric orbits, and monitor the rate at which this quantity converges to zero. For large values of p, the actual period data are discarded, to reduce the size of the output data files.

From lemma 1, to obtain a complete representation of parameter space for given p, it suffices to consider the restricted range

$$0 \leqslant \alpha < \lfloor p/2 \rfloor \qquad\qquad 0 \leqslant \beta < p-1.$$

4.1. **Convergence to the gamma-distribution.** An overview of the behaviour of the function $\mathcal{E}_p(\alpha,\beta)$ over the entire parameter space is given in figure 1. These data, and all the data in the rest of the paper, correspond to the scaling constant $\kappa = \bar{t}$ —see equation (8). Each pixel in the figure represents a pair (α,β), and the value of $\mathcal{E}_p(\alpha,\beta)$ is encoded on a grey scale. The larger the deviation from the gamma-distribution, the darker the pixel. Thus the white areas correspond to small values of $\mathcal{E}$, which indicate proximity to $\mathcal{R}$, while the black pixels represent the largest deviations.

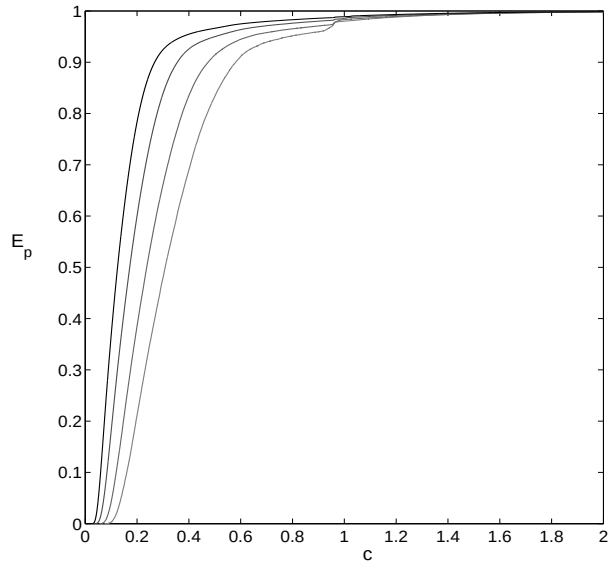

Figure 2: The function $E_p(c)$ —see equation (16)— for $p = 251, 499, 1103, 2339$ (right to left). As p increases, we see non-uniform convergence of $E_p(c)$ to 1, supporting conjecture 1.

Before examining the nature of the large deviations from the gamma-distribution, we consider the typical behaviour of the distribution function, using the construct developed in

section 3. In figure 2, we show the function $E_p(c)$, for three increasing values of p. Details of this figure are displayed in figure 3, showing the behaviour near the origin and near the top. Near the origin, the empirical distribution remains zero (or very small) over a gradually shrinking interval. At the same time, the graph of E_p raises towards 1, while anomalies are smoothed out. In addition (not evident from the picture), the smallest value of c for which $E_p(c) = 1$ migrates to the right (see below). These data provide convincing evidence for the convergence of E_p to 1, which is conjecture 1. The overall rate of convergence is slow —approximately logarithmic in p.

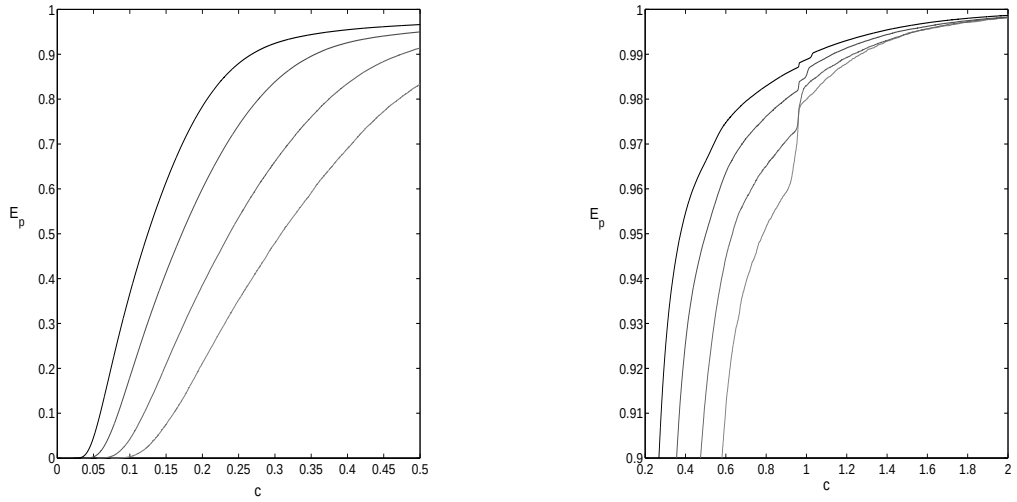

Figure 3: Details of figure 2. Left: the behaviour of $E_p(c)$ near the origin. Right: behaviour near the top.

Large deviations from the gamma-distribution originate from two distinct phenomena, which we describe in the next two sections.

4.2. **Anomalous sectors.** Experimental data show that there are anomalous distributions in the vicinity of many low-order (i.e., small denominator) rational parameter pairs, which we call *cluster points*. The most prominent cluster points are $(0, 0)$ and $(1/2, 1/2)$ but several others are visible elsewhere (see figure 1). However, cluster points are missing at some low-order rational parameters, such as those of the form $(0, m/n)$, with even n.

To each cluster point we associate two rational lines, one with positive slope, and one with negative slope. These lines divide the neighbourhood of a cluster into four *sectors* (taking into account the periodicity of parameter space, if necessary). For instance, the sectors of the clusters at $(0, 0)$ and $(1/2, 1/2)$ are determined by the lines with slope ± 1.

Details of the clusters points at $(0, 0)$ and $(1/4, 1/4)$ are shown in figure 4. The behaviour of $\mathcal{E}$ changes markedly and abruptly from sector to sector. The East and West sectors, which we call the *anomalous sectors,* feature deviations from the gamma-distribution which are not only larger in value, but which also affect a two-dimensional region in parameter space. By contrast, the large fluctuations within the North and South sectors —the *regular sectors*— are confined to one-dimensional rational lines (see below).

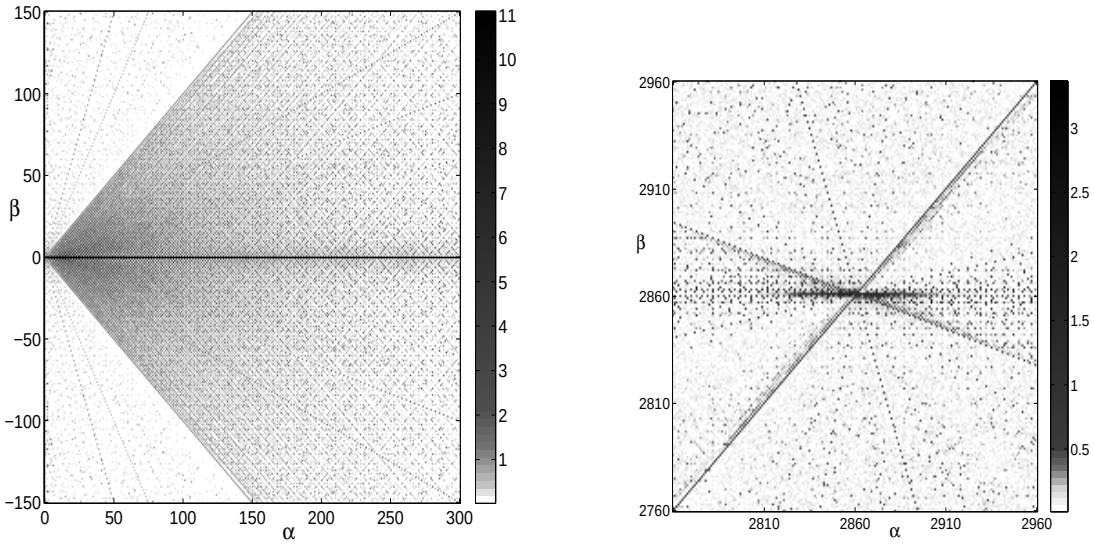

Figure 4: Details of the anomalous sectors of two cluster points. The values of the function $\mathcal{E}_p(\alpha, \beta)$, are represented on a grey scale, with the largest values in black. Left: the sectors of the cluster point $(\alpha, \beta) = (0, 0)$, for $p = 9011$. Right: the sectors of the cluster point $(1/4, 1/4)$, but now shown for the larger prime $p = 11433$.

Thus, near the $(0, 0)$ cluster point, convergence to the gamma-distribution is much faster for $|\beta| > |\alpha|$ than for $|\beta| \leqslant |\alpha|$. Within the former domain, the lines $\alpha = 0$ and $3\alpha = \pm\beta$ feature the most prominent fluctuations, while all other rational lines give much smaller deviations. On the other hand, within the anomalous sector $|\beta| \leqslant |\alpha|$, large deviations are found to occur for even values of $\gamma = \alpha + \beta$. There are also large fluctuations on rational lines, most notably, the lines $\beta = 0$ and $|\beta| = \alpha/3$.

In the anomalous sectors, a mechanism is at work, which delays convergence of averages. In order to reconcile these findings with the data shown previously, we provide evidence that these fluctuations do indeed decay to zero, as $p \to \infty$. In figure 5, we compare the value of $\mathcal{E}_p$ in the anomalous and regular sectors near $(0, 0)$, for increasing values of p. To isolate the dominant features, we perform a double average. First, we average $\mathcal{E}_p$ over the lines $\gamma = const$ (cf. equation (5)), because we found that the variations of $\mathcal{E}$ are much stronger along the orthogonal coordinate δ. Thus, inside the anomalous sector, we compute

$$\bar{\mathcal{E}}_\gamma = \frac{1}{n} \sum_{\alpha=1}^{n} \mathcal{E}_p(\alpha, \gamma - \alpha) \qquad n(\gamma) = \left\lfloor \frac{\gamma - 1}{2} \right\rfloor .$$

(The quantity $\mathcal{E}_p(\gamma - \alpha, \alpha)$ is used for the regular sector.) Then we perform a Cesaro sum over γ

$$\langle \mathcal{E} \rangle_\gamma = \frac{1}{\gamma - 2} \sum_{\gamma'=3}^{\gamma} \bar{\mathcal{E}}_{\gamma'}. \tag{35}$$

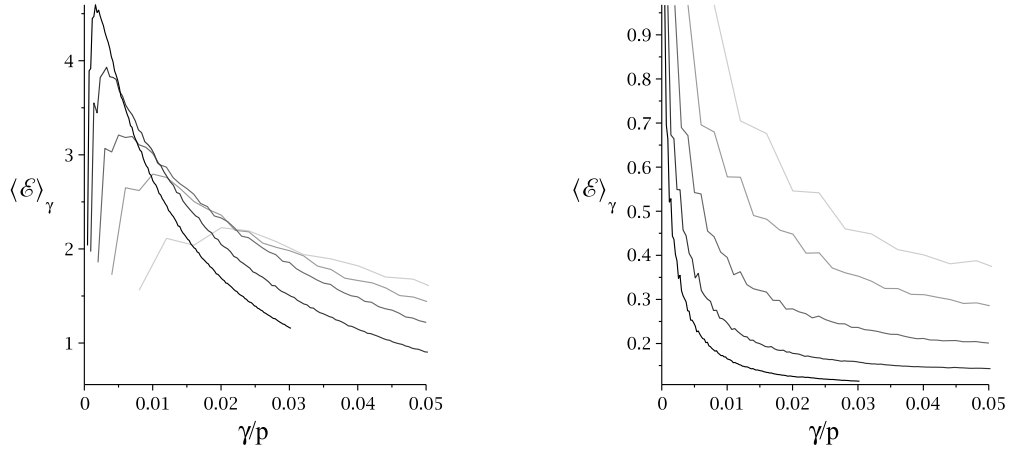

Figure 5: Left: Non-uniform convergence to the gamma-distribution for parameters pairs (α, β) within an anomalous sector of the cluster point $(0, 0)$ $(0 < \beta < \alpha)$. The five curves in increasing darkness correspond to the primes $p = 499, 997, 1999, 4297, 8599$. In each case we plot the Cesaro sum $\langle \mathcal{E} \rangle_\gamma$, given in equation (35), as a function of γ/p for even values of γ (the odd values of γ give much lower values of $\bar{\mathcal{E}}_\gamma$). Right: the same functions, within the regular sector $(0 < \alpha < \beta)$.

As p increases, the function $\langle \mathcal{E} \rangle_\gamma$ develops a singular profile within the anomalous sector, within an overall logarithmic convergence to zero. This behaviour is indeed consistent with the validity of conjecture 1, but it suggests that the smallest value of c for which $E_p(c) = 1$, diverges to infinity, as $p \to \infty$. Equivalently, there exist sequences of rational parameter values, converging to $(0, 0)$, along which the distance from the gamma-distribution diverges to infinity. These anomalous distributions are dominated by the presence of few very large cycles.

4.3. **Singular distributions on rational lines.** A second source of large fluctuations are anomalous distributions along lines with rational slope, the most prominent of which are

$$\beta = \pm\alpha, \quad \beta = \pm 3\alpha.$$

On these lines the distribution function has a step-like behaviour, which accounts for the large value of $\mathcal{E}$.

There are in fact singular distributions on all parametric lines of the form $\beta = k\alpha$. The corresponding empirical distributions are defined as

$$\mathcal{R}^{(k)}_{p,\alpha}(x) := \mathcal{D}_{p,\alpha,k\alpha}(x) \tag{36}$$

where $\mathcal{D}$ was defined in (6), and the parameter dependence has been made explicit (see also equation (32)). Some empirical singular distribution are plotted in figure 6. The conjectured analytical form $\mathcal{R}^{(k)}$ of the distributions corresponding to even values of k is given in equation (31). These functions have been determined by trial and error, examining empirical distributions for large primes.

Our experiments show that there are analogous distributions on prime lattices also for odd k. However, apart from the values $k = 1, 3$, we could only locate the singularities of these distributions, but not their analytical form. The empirical distributions for $k = 1, 3, 5$ are

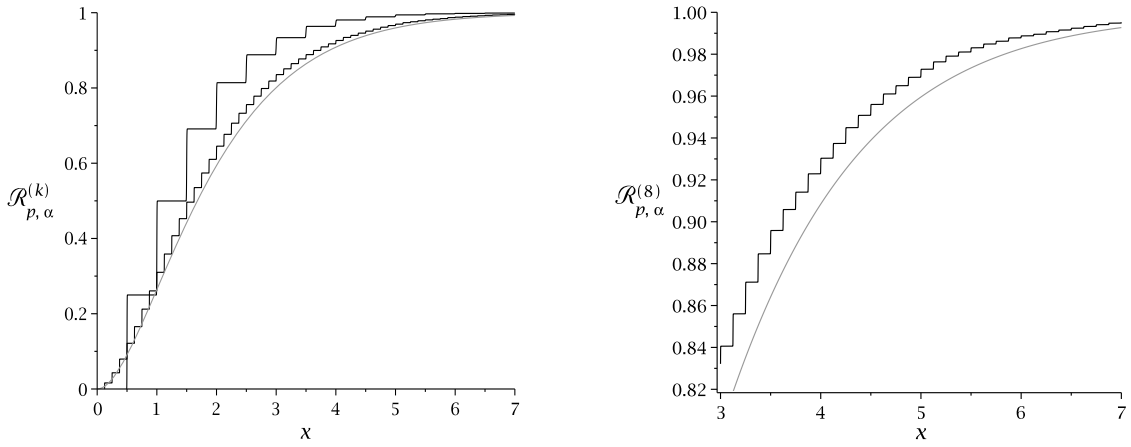

Figure 6: Empirical period distribution functions $\mathcal{R}^{(k)}_{p,\alpha}$ on rational lines $\beta = k\alpha$, for even k. Left: for the prime $p = 81799$ and $\alpha = 70$, we display the distributions for $k = 2$ (large steps) and $k = 8$ (small steps). The smooth curve is the gamma-distribution. Right: blow-up of the fine structure of the function $\mathcal{R}^{(8)}_{p,\alpha}$, in the range $3 \leqslant x \leqslant 7$, showing the 32 steps predicted by formula (31). Again, the smooth curve is the gamma-distribution.

given in figure 7. Of note is the fact that $\mathcal{R}^{(1)}_{p,\alpha}$ and $\mathcal{R}^{(3)}_{p,\alpha}$ have finitely many steps; by contrast $\mathcal{R}^{(5)}_{p,\alpha}$ appears to have infinitely many steps at the integer multiples of $2/5$, although the value of the heights of the steps is not obvious.

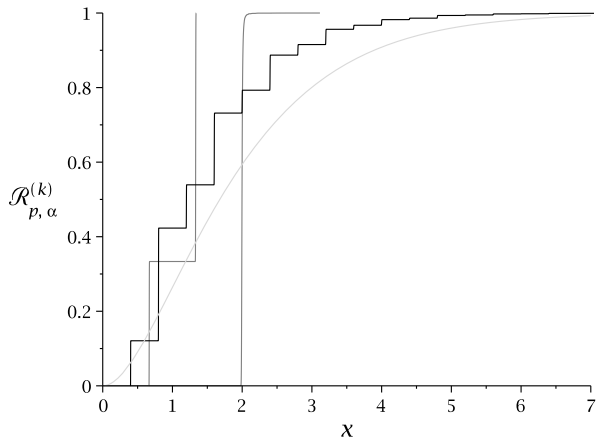

Figure 7: Empirical period distribution functions $\mathcal{R}^{(k)}_{p,\alpha}$ on rational lines $\beta = k\alpha$, for odd k. For the prime $p = 81799$ and $\alpha = 5$, we display the empirical distributions for $k = 1$ (one step), $k = 3$ (two steps), and $k = 5$ (several steps). The smooth curve is the gamma-distribution.

The result for $k = 1, 3$ is given by the following

Conjecture 4. *In the limit of large primes p, and independent of α, the empirical period distribution $\mathcal{R}^{(k)}_{p,\alpha}$ for the Casati-Prosen map with parameters $\beta = k\alpha$, for $k = 1$ and $k = 3$ converges, respectively, to the functions*

$$\mathcal{R}^{(1)}(x) = \begin{cases} 0 & \text{if } x < 2 \\ 1 & \text{if } x \geqslant 2 \end{cases} \qquad \mathcal{R}^{(3)}(x) = \begin{cases} 0 & \text{if } x < \frac{2}{3} \\ \frac{1}{3} & \text{if } \frac{2}{3} \leqslant x < \frac{4}{3} \\ 1 & \text{if } \frac{4}{3} \leqslant x. \end{cases} \tag{37}$$

In figure 8 we analyse the emergence of the singularity at $x = 2$ for the distribution $\mathcal{R}^{(1)}_{p,\alpha}$, for two primes and a sample of values of α. The build-up of the step in the distribution function is quite regular, and seems to be optimal for $\alpha = 1$.

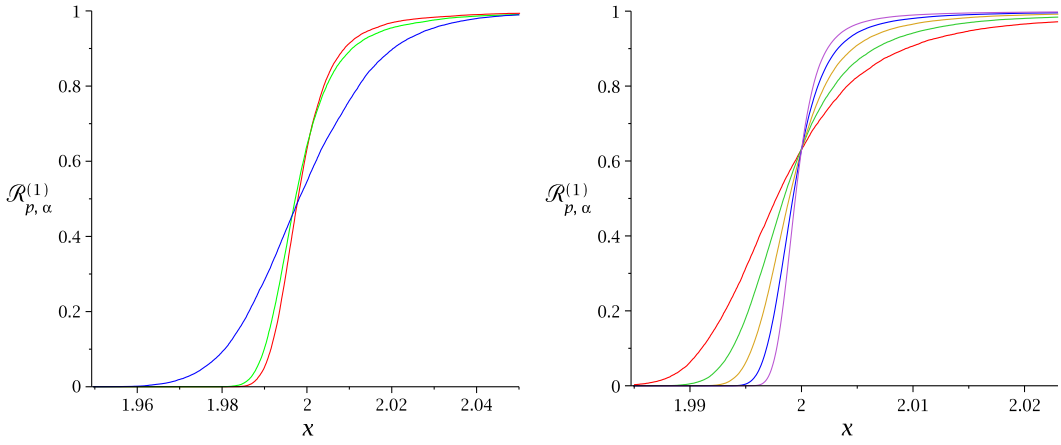

Figure 8: Convergence of the empirical distribution $\mathcal{R}^{(1)}_{p,\alpha}$ to $\mathcal{R}^{(1)}$ ($\beta = \alpha$), in the proximity of the step at $x = 2$. Left: The prime $p = 53993$ is fixed and shown are the distributions for $\alpha = 1, 2, 23936$. The steepest curves correspond to the values $\alpha = 1, 2$. Right: Shown are the distributions $\mathcal{R}^{(1)}_{p,\alpha}$ for fixed $\alpha = 1$ and the sequence of primes $p = 50021, 100043, 200023, 400033, 800077$. The convergence to the step function improves with the prime.

To gain an overview of this phenomenon, we plot the value of the norm $\mathcal{E}^{(k)}_p(\alpha)$ ((32) with (36)) for two large primes p, for $k = 1$ and $k = 3$, over the full range of α values (figure 9). The convergence of the empirical distributions $\mathcal{R}^{(k)}_{p,\alpha}$ to their conjectured value (37) is noticeably faster for $k = 3$ (and, in both cases, roughly algebraic in p, with exponent close to $-1/2$). Convergence is uniform in α, and the data show evidence of scaling in the fluctuations. For $k = 1$, the fastest convergence takes place near the endpoints of the line, which are the cluster points $(0, 0)$ and $(1/2, 1/2)$.

4.4. **Asymmetric orbits.** In this section we test the validity of conjecture 3. From the knowledge of the periods of all symmetric orbits, one determines the value of the expression $\mathcal{A}_p(\alpha, \beta)$ for the desired set of parameters.

Numerical experiments show that, much like for the distance from the gamma-distribution, the proportion of asymmetric periodic orbits is small on average, but also far from uniform in parameter space. We first consider the distribution function $A_p(c)$, defined in equation (34). In figures 10 and 11, we show the empirical function $A_p(c)$, for three increasing values of p.

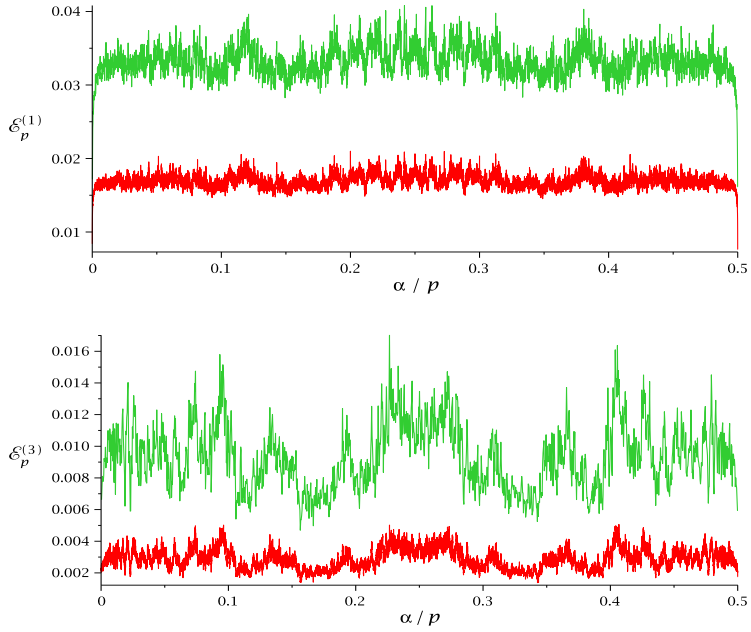

Figure 9: In the top figure, we plot the norm $\mathcal{E}_p^{(1)}(\alpha)$ as a function of $\alpha/p \in [0, \frac{1}{2}]$ for the primes $p = 7699$ and $p = 33521$, the latter giving the smaller norm. In the bottom figure, we plot the norm $\mathcal{E}_p^{(3)}(\alpha)$ as a function of α/p for the primes $p = 2927$ and $p = 33521$. The convergence for $\mathcal{E}_p^{(3)}(\alpha)$ is noticeably better than for $\mathcal{E}_p^{(1)}(\alpha)$.

As for E_p, the convergence to 1 is non uniform, and approximately logarithmic. Note that, as p increases, the value of $A_p(0)$ decreases, because, due to the improved statistics, a small number of asymmetric orbits appears for an increasing fraction of parameter values.

Figure 12 is the analogue of figure 1 for asymmetric orbits, The function $\mathcal{A}_p(\alpha, \beta)$ is coded on a grey scale, The zones with the highest proportion of asymmetric orbits, the darkest pixels, form anomalous sectors, which develop around cluster points. The structure of the function $\mathcal{A}_p$ is similar to that of $\mathcal{E}_p$, with two important differences. First, the rational lines are not anomalous. Second, the anomalous sectors include sectors which are not anomalous for $\mathcal{E}_p$, such as those of the form $(0, m/n)$, with even n.

The neighbourhood of the $(0, 0)$ cluster is shown in figure 13, for the prime $p = 8599$. The structure is rather similar to that of figure 4, even though the boundary of the anomalous sector seems somewhat shifted away from the line $\alpha = \beta$. Finally, in figure 14, the analogue of figure 5, we compare the value of $\mathcal{A}_p$ in the anomalous and regular sectors near $(0, 0)$, for increasing values of p. The averaging procedure to determine $\langle \mathcal{A} \rangle_\gamma$ is the analogue of that described by equation (35).

5. Concluding remarks

Our study of the C-P map provides further evidence of the ubiquity and universality of the gamma-distribution (7) for periodic orbits of reversible maps. This asymptotic distribution had not been previously observed on a zero-entropy map, and it seems to require milder

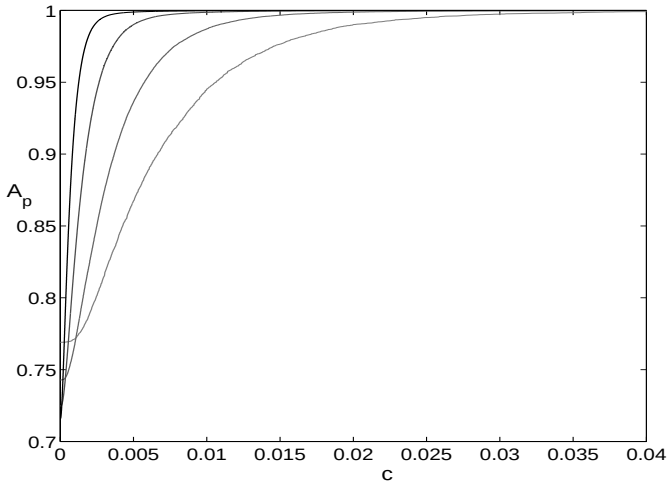

Figure 10: Details of the functions $A_p(c)$ —see equation (34)— near the origin, for $p = 251, 499, 1103, 2339$ (right to left). As p increases, we see non-uniform convergence of $A_p(c)$ to 1, supporting conjecture 3.

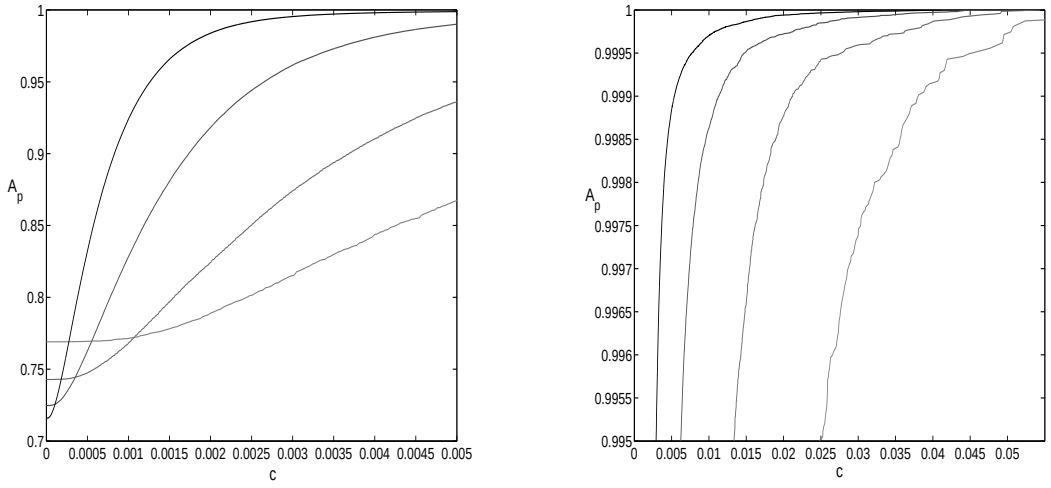

Figure 11: Details of figure 10. Left: the behaviour of $A_p(c)$ near the origin. Right: behaviour near the top.

ergodic properties than originally thought. We have also shown that, within the same two-parameter family of maps, it is possible to observe a transition from singular distributions to the gamma distribution.

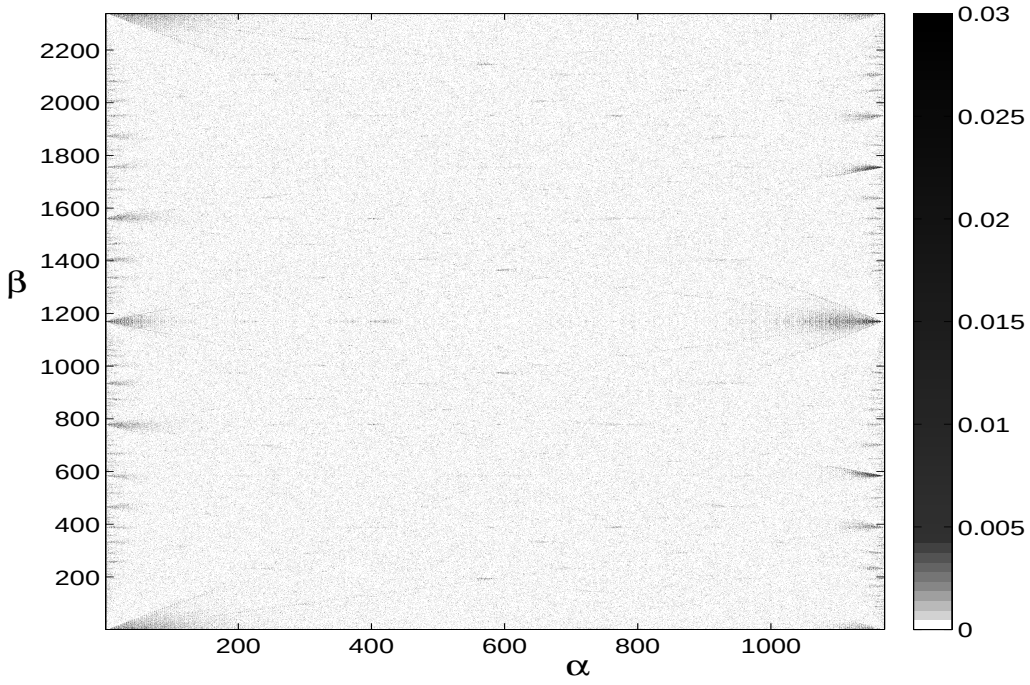

Figure 12: Parameter dependence of the function $\mathcal{A}_p(\alpha, \beta)$ (equation (34)) for $N = p = 2339$, a prime number. The value of $\mathcal{A}_p$ is coded on a grey scale, the darker a pixel, the larger the fraction of asymmetric orbits at the corresponding parameter pair (α, β).

The restriction to prime lattices has been necessary to obtain well-behaved singular distributions $\mathcal{R}^{(k)}$ along rational lines. For composite values of N, we have found examples in which both the location and the height of the steps differed from those of prime lattices.

Many questions raised by our findings remain unanswered, the main issue being a rigorous justification of the asymptotic emergence of the gamma-distribution. Another intriguing problem is the identification of the mechanism responsible for slow convergence to averages in the anomalous sectors of parameter space. Within these sectors we observe a large variety of orbit distributions, which differ considerably from the singular distributions seen on rational lines.

The conjectured form of singular distributions $\mathcal{R}^{(k)}$ is attractively simple, yet at present we have no rigorous explanation of their origin. We note that singular period distributions often have an arithmetical characterisation. We have pointed out that in the case of toral automorphisms, the singular behaviour results from the presence of abelian groups, whose normalised order depend on the prime factorisation of the lattice size N. Singular distributions also appear for integrable rational maps acting over finite fields [15, 6]. The underlying abelian groups now are addition over the elliptic curves that foliate the phase space. The Hasse-Weil bound ensures that, asymptotically, the normalised order of these groups is the same, leading again to steps in the period distribution function.

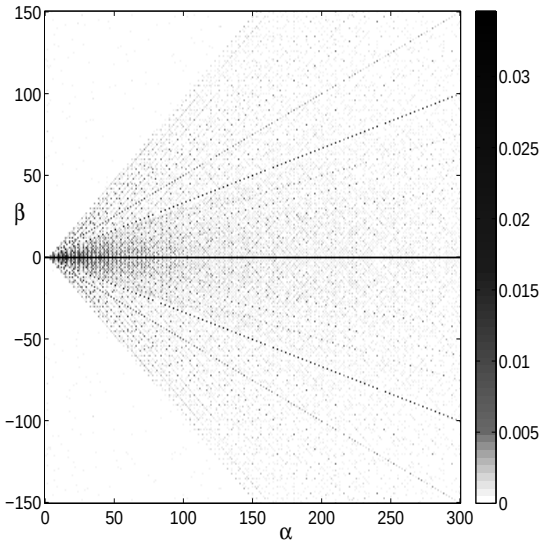

Figure 13: Details of the parameter dependence of the function $\mathcal{A}_p(\alpha, \beta)$, for the prime $p = 9011$, in the vicinity of the origin. The darker dots represent the parameter pairs corresponding to a relatively large proportion of asymmetric orbits. The corresponding picture for $\mathcal{E}_p(\alpha, \beta)$ for this prime was shown in the left frame of figure 4.

From an ergodic-theoretic viewpoint, all phenomena described in this work refer to exceptional values, both in parameter space, and in phase space. However, looking at rationals in order to understand irrationals is natural, and it is quite possible that our findings are the manifestation of phenomena that concern generic parameter values as well.

Acknowledgements: This work was inspired by a talk given by Mirko degli Esposti in Trieste. We are grateful to Martin Horvat for generously sharing with us some preliminary data on period distribution of the triangle map. The very detailed comments of one referee did much to improve the accuracy and clarity of this paper. JAGR and FV would like to thank, respectively, the School of Mathematical Sciences at Queen Mary, University of London, and the School of Mathematics and Statistics at the University of New South Wales, Sydney, for their hospitality. This work was supported by the Australian Research Council.

References

[1] A. Avila and G. Forni, Weak mixing for interval exchange transformations and translation flows, *Ann. Math.* **165** (2007) 637–664.

[2] M. Baake and J.A.G. Roberts, The structure of reversing symmetry groups, *Bull. Austral. Math. Soc.* **73** (2006) 445–459.

[3] G. Casati and T. Prosen, Triangle map: A model for quantum chaos, *Phys. Rev. Lett.* **85** (2000) 4261–4264.

[4] R. De Vogelaere, On the structure of symmetric periodic solutions of conservative systems, with applications, in: *Contributions to the Theory of Nonlinear Oscillations, Vol. 4*, ed. S. Lefschetz, Princeton University Press, Princeton (1958), pp. 53-84.

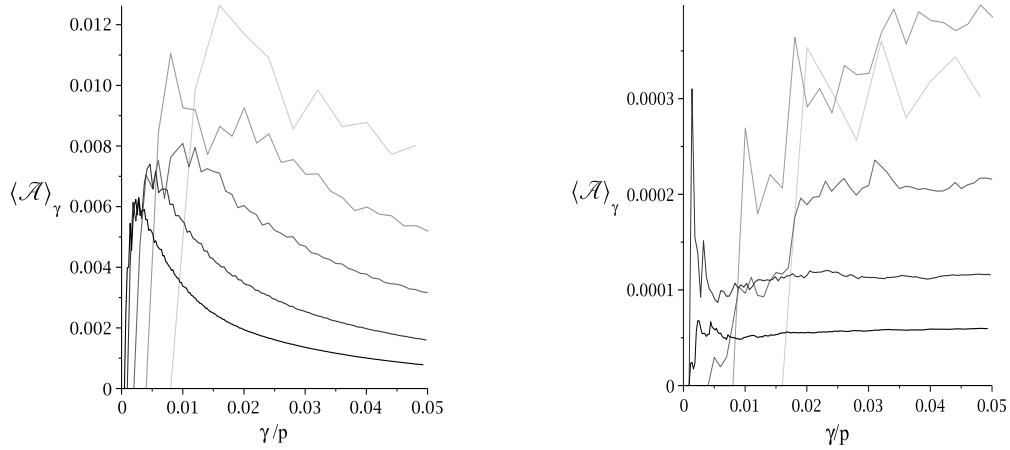

Figure 14: Left: Analogous to figure 5, but now considering proportion of asymmetric periodic points for parameters pairs (α, β) within an anomalous sector of the cluster point $(0, 0)$ $(0 < \beta < \alpha)$. The five curves in increasing darkness correspond to the primes $p = 499, 997, 1999, 4297, 8599$. In each case we plot the Cesaro average $\langle \mathcal{A} \rangle_\gamma$ of $\mathcal{A}_p(\alpha, \beta)$, over the parameter pairs satisfying $\alpha + \beta = \gamma$, as a function of γ/p. The dominant contribution to the nature of each curve comes again from the even values of γ, whereas averages over odd values of γ give systematically lower values of $\langle \mathcal{A} \rangle_\gamma$. Right: the same functions, within the regular sector $(0 < \alpha < \beta)$.

[5] J. M. Finn, PhD Thesis, University of Maryland (1974).
[6] D. Jogia, J. A. G. Roberts, and F. Vivaldi, Algebraic geometric approach to integrable maps of the plane, *J. Phys. A* **39** (2006) 1133–1149.
[7] G. H. Hardy ang E. M. Wright, *An introduction to the theory of numbers,* Oxford University Press, Oxford (1979).
[8] M. Horvat, M. Degli Esposti, S. Isola, T. Prosen, and L. Bunimovich, On ergodic and mixing properties of the triangle map, *Physica D* **238** (2009) 395–415.
[9] R. V. Hogg and A. T. Craig, *Introduction to Mathematical Statistics,* 4th edition, Macmillan, New York (1978).
[10] J. S. W. Lamb and J. A. G. Roberts, Time-reversal symmetry in dynamical systems: A survey, *Physica* **D 112** (1998) 1–39.
[11] R.S. MacKay, *Renormalisation in Area-Preserving Maps*, World Scientific, Singapore, 1993.
[12] N. Neumärker, J. A. G. Roberts, C.-M. Viallet, and F. Vivaldi, in preparation.
[13] I. Percival and F. Vivaldi, Arithmetical properties of strongly chaotic motions, *Physica D* **25** (1987) 105–130.
[14] J. A. G. Roberts and G. R. W. Quispel, Chaos and time-reversal symmetry — order and chaos in reversible dynamical systems, *Phys. Rep.* **216** (1992) 63–177.
[15] J. A. G. Roberts and F. Vivaldi, Arithmetical Methods to detect integrability in maps, *Phys. Rev. Lett* **90** 3 (2003) [034102].
[16] J. A. G. Roberts and F. Vivaldi, Signature of time-reversal symmetry in polynomial automorphisms over finite fields, *Nonlinearity* **18** (2005) 2171–2192.
[17] J. A. G. Roberts and F. Vivaldi, A combinatorial model for reversible rational maps over finite fields, *Nonlinearity* **22** (2009) 1965–1982.
[18] X-S Zhang and F Vivaldi, Small pertubations of a discrete twist map, *Ann. Inst. Henry Poincare* **68** (1998) 507–523.

School of Mathematics and Statistics, University of New South Wales, Sydney, NSW 2052, Australia
E-mail address: n.neumaerker@unsw.edu.au

School of Mathematics and Statistics, University of New South Wales, Sydney, NSW 2052, Australia
E-mail address: jag.roberts@unsw.edu.au
URL: http://www.maths.unsw.edu.au/~jagr

School of Mathematical Sciences, Queen Mary, University of London, London E1 4NS, UK
E-mail address: f.vivaldi@maths.qmul.ac.uk
URL: http://www.maths.qmul.ac.uk/~fv